Landau-Zener-Stückelberg interferometry in the presence of quantum noise

Lingjie Du, Minjie Wang, and Yang Yu*
National Laboratory of Solid State Microstructures and Department of Physics, Nanjing University, Nanjing 210093, China
(Received 14 May 2010; published 30 July 2010)

We proposed an unconventional Landau-Zener-Stückelberg interferometry in strongly driven two-level systems subjected to quantum noise. A general transition rate for consecutive Landau-Zener transitions was obtained, from which we could analytically calculate interference fringes. The strong low-frequency noise would detour the evolution paths, leading to asymmetric transition rates which caused unpredicted position shift of the fringes and population inversions in a two-level system.

DOI: 10.1103/PhysRevB.82.045128 PACS number(s): 03.65.Yz, 03.67.Lx, 74.50.+r, 85.25.Cp

The model of quantum two-level systems (TLSs) is used to describe various physical systems. When a TLS is subject to strong periodic driving, consecutive transitions between energy levels at an avoided crossing (known as Landau-Zener transition) occur. The phase accumulated between transitions may result in Landau-Zener-Stückelberg (LZS) interferometry,[1] which is demonstrated in a variety of systems.[2] Recently, increasing attention has been paid on LZS interferometry in superconducting qubits in which the interferometry serves as an effective tool for obtaining the parameters characterizing the qubit as well as its interaction with the control fields and with the environment.[3–7] Moreover, strong driving could allow for fast and reliable control of the qubits, paving a way of demonstration of macroscopic quantum coherence and implementation of practical quantum processor.[8–10]

In order to demonstrate LZS interferometry, one applies microwaves with large amplitude to the superconducting qubits which can be considered as artificial two-level systems. The superconducting qubits undergo repeated LZ transitions[11] at the avoided crossing, which act as coherent beam splitters to separate the state into two evolution paths. The phase accumulated from two paths coherently interfere each other, leading to an oscillatory dependence of qubit population in the final state on the detuning from the avoided crossing (or degeneracy point) and the driving amplitude.

The observed conventional LZS interferometry was addressed with LZ transition theory considering either no noise or classical noise.[2,3,5] However, the superconducting flux qubits usually couple with their environment very strongly. A variety of noises may produce unexpected interference features. For instance, it was found that the dephasing can wash out the interference patterns by widening resonant peaks. In order to obtain resolvable interference fringes, one needs to use microwave with frequencies larger than the dephasing rate Γ_2.[5,12] In this work, we studied LZS interferometry of a strongly driven superconducting flux qubit in the quantum noise environment. For a dc flux bias close to $\Phi_0/2$, the flux qubit exhibits a double-well energy landscape. Since the dephasing rate is usually larger than the tunneling couple Δ between the diabatic levels in the opposite wells, we consider that the microwave frequency is always larger than Δ, resulting Mach-Zehnder-type LZS interferometry.[3] In addition, the energy spacing between the diabatic levels localized in each well, which is on the order of the plasma frequency ω_p, is much larger than Δ. In the presence of frequency-dependent noise, a phase factor may be built up in the transition rate, detouring the original evolution paths and leading to unconventional LZS interferometry with a shift of the resonant conditions. In addition, quantum noise from environment can generate stationary population inversion between only two qubit levels through LZ transitions. This noise-generated population inversion in TLS is not predicted by previous theory, although population inversion has been demonstrated for a long time in superconducting devices[6,7,13–16] and quantum-dot system.[17,18] This model can also be applied to other two-level systems in the presence of the quantum noise.

We start from a two-level system consisting of the two lowest diabatic levels $|1\rangle$ and $|0\rangle$ in the left and right well coupled with an environment bath (Fig. 1). Such system can be described by the Hamiltonian (we set $\hbar=k_B=1$),

$$H_1 = -\frac{\Delta}{2}\sigma_x - \frac{\varepsilon(t)}{2}\sigma_z - \frac{Q}{2}\sigma_z + \chi\sigma_x + H_B, \tag{1}$$

where Δ is the tunnel coupling between $|1\rangle$ and $|0\rangle$, σ_x and σ_z are Pauli matrices. $\sigma_z=|1\rangle\langle 1|-|0\rangle\langle 0|$. H_B is the environment's Hamiltonian and Q is quantum noise operator acting on the environment. $\varepsilon(t)=\varepsilon_0+A\cos(\omega t)$ is the energy detuning from the avoided crossing, where ε_0 is the dc component of the energy detuning, A and ω are the amplitude and frequency of the microwave, respectively, and the term $\chi\sigma_x$ expresses the relaxation process between two lowest levels.

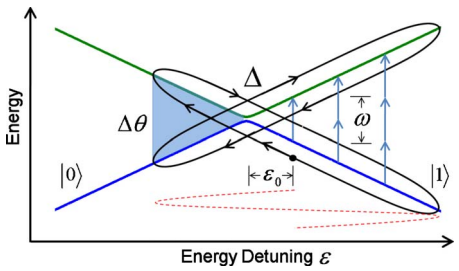

FIG. 1. (Color online) Schematic energy diagram of a two-level system. The periodic driving field $A\cos\omega t$ sweeps the system through the avoided crossing repeatedly, building a relative phase difference $\Delta\theta$ (shade area) which results conventional Landau-Zener-Stückelberg interference between $|0\rangle$ and $|1\rangle$. The vertical solid arrows mark the resonant condition $n\omega=\varepsilon_0$ for the stationary population transition.

First of all we calculate the LZ transition rate between two lowest levels in the long system dynamics time $t \gg 1/\Gamma_2$ by ignoring the relaxation term between two levels since it is very small [We will involve the relaxation in Eq. (11) when discuss the system dynamics.]. We take an interaction picture with respect to H_B and then rewrite the Hamiltonian in the rotating frame where $\mathcal{T}\exp\{i/2\int_0^t[Q(\tau)+\varepsilon(\tau)]\sigma_z d\tau\}|\psi\rangle \to |\psi\rangle$ ($|\psi\rangle$ is the state vector in the laboratory frame),

$$H_2(t) = -\frac{\Delta}{2}U(t)U_+^\dagger(t)U_-(t)|1\rangle\langle 0| + \text{H.c.}, \tag{2}$$

where $Q(t)=e^{iH_Bt}Qe^{-iH_Bt}$, $U(t)=\mathcal{T}\exp[-i/2\int_0^t\varepsilon(\tau)d\tau]$, and $U_\pm(t)=\mathcal{T}\exp[\pm(i/2)\int_0^t Q(\tau)d\tau]$ with $\mathcal{T}$ expressing the time ordering. It should be noticed that after the rotating transformation the qubit states $|1\rangle$ and $|0\rangle$ contain a phase factor which has no contribution to any observable. Comparing with the Hamiltonian of the general two-level system,[2] we have extra factor $U_+^\dagger(t)U_-(t)$, which can lead interesting phenomena because of the coupling to many degrees of freedom of the environment.

When the LZ transition rate between $|1\rangle$ and $|0\rangle$ is much less than W, which is the noise induced resonant width and represents the dephase rate Γ_2,[19] we can calculate the LZ transition rate in the perturbation theory by treating the Hamiltonian H_2 as perturbation. Averaging over all environment mode, we obtain the LZ transition rate from the state $|0\rangle$ to $|1\rangle$:

$$W_{01}(t) = \frac{dP(t)}{dt},$$

$$P(t) = \left\langle \int_0^t dt_1 \int_0^t dt_2 \langle 0|H_2(t_2)|1\rangle\langle 1|H_2(t_1)|0\rangle \right\rangle. \tag{3}$$

Here $\langle\cdots\rangle \equiv \mathrm{Tr}_B\{\rho_B\ldots\}$, ρ_B is the density matrix of the environment in equilibrium. Then we introduce the relationship $e^{-i(A/\omega)\sin\omega t}=\Sigma J_n(A/\omega)e^{i\omega nt}$. For $\omega \gg \Delta$, the nonresonant exponent terms caused by Bessel function oscillate very fast compared to the long time scale of the dynamics. The effect of the nonresonant terms can therefore be neglected for the long-time system dynamics. In this case, we can evaluate,

$$P(t) = \frac{\Delta^2}{4}\sum_n J_n^2(A/\omega)\int_0^t dt_1\int_0^t dt_2 e^{i(\varepsilon_0-n\omega)(t_2-t_1)} \times \langle U_-^\dagger(t_2)U_+(t_2)U_+^\dagger(t_1)U_-(t_1)\rangle. \tag{4}$$

We assume the environment bath can be described by the Gaussian distribution. Therefore, all average can be expressed by the spectral density of the noise $Q(t)$, which is defined as $S(\omega')=\frac{1}{2\pi}\int_{-\infty}^{\infty}dt e^{i\omega' t}\langle Q(t)Q(0)\rangle$. For classical noise, $S(\omega')=S(-\omega')$ while for quantum noise $S(\omega')\neq S(-\omega')$. Then we can calculate the correlation function in Eq. (4) by expanding $U_\pm(t)$ to the second order in $Q(t)$, averaging and exponentiating the result. That gives

$$\langle U_-^\dagger(t_2)U_+(t_2)U_+^\dagger(t_1)U_-(t_1)\rangle \approx \exp\left\{\frac{1}{2}\int_{t_2}^{t_1}dt''\left[\int_0^{t_2}dt'\langle Q(t')Q(t'')\rangle - \int_0^{t_1}dt'\langle Q(t'')Q(t')\rangle\right]\right\}. \tag{5}$$

With the spectral density $S(\omega')$, we can simplify Eq. (5) as

$$\langle U_-^\dagger(t_2)U_+(t_2)U_+^\dagger(t_1)U_-(t_1)\rangle \approx \exp\left\{\int d\omega' S(\omega')\frac{e^{-i\omega'\tau}-1+i2\sin\frac{\omega'\tau}{2}\cos\omega' t'}{\omega'^2}\right\},$$

where $\tau=t_2-t_1$ and $t'=(t_2+t_1)/2$. Then we can change Eq. (4) to

$$P(t) \approx \frac{\Delta^2}{4}\sum_n J_n^2\left(\frac{A}{\omega}\right)\int_0^t dt'\int_{-\tilde{t}}^{\tilde{t}}d\tau e^{i(\varepsilon_0-n\omega)\tau} \times \exp\left\{\int d\omega' S(\omega')\frac{e^{-i\omega'\tau}-1+i2\sin\frac{\omega'\tau}{2}\cos\omega' t'}{\omega'^2}\right\},$$

where $\tilde{t}=\min[2t',2(t-t')]$. With Eq. (3), we obtain[20]

$$W_{01}(t) \approx \frac{\Delta^2}{4}\sum_n J_n^2\left(\frac{A}{\omega}\right)\int_{-t}^{t}d\tau e^{i(\varepsilon_0-n\omega)\tau} \times \exp\left\{\int d\omega' S(\omega')\frac{e^{-i\omega'\tau}-1+i2\sin\frac{\omega'\tau}{2}\cos\omega' t}{\omega'^2}\right\}. \tag{6}$$

This is the general LZ transition rate in strong driving with high-frequency microwave under environment noise. Similarly, we can calculate $W_{10}(\varepsilon_0)=W_{01}(-\varepsilon_0)$. From Eq. (6), we know that the contributions mainly come from the low-frequency part of the environment noise. Under the stationary condition, the time scale of the dynamics t is large rela-

tively to $1/W$. In this case, if the noise is frequency independent (white) in low-frequency regime $\omega'/2\pi \lesssim 1/t$ (Ref. 21) which has $S(\omega') \approx S(0)$, we can extend the integration boundaries of Eq. (6) to ∞ and integrate it, obtaining the LZ transition rate described by the sum of the Lorentzian-shaped n-photons resonance,

$$W_{01} = \frac{\Delta^2}{2}\sum_n \frac{W J_n^2\left(\frac{A}{\omega}\right)}{(\varepsilon_0 - n\omega)^2 + W^2}, \quad W = \pi S(0). \tag{7}$$

This exactly describes the conventional LZS interference with the same result of classical noise model[5] so as to verify our theory. From Eq. (7), the effect of the classical noise is widening the resonant peaks thus smearing the interference patterns.

Much more interesting phenomena can be observed with presence of the frequency-dependent strong low-frequency noise. If the noise is dominated by $1/\omega'$ spectral in low-frequency part $\omega' \ll 1/\tau$ in Eq. (6) (i.e., the noise is strong in the low-frequency regime), we only need to consider the first three terms from the power series expansion in $\omega'\tau$ in Eq. (6). When $t \gg 1/W$ and $S(\omega')$ is asymmetric in ω', we can change Eq. (5) into

$$\langle U_-^\dagger(t_2)U_+(t_2)U_+^\dagger(t_1)U_-(t_1)\rangle \approx \exp\{i\varepsilon_p(t)(t_2 - t_1) - W^2(t_2 - t_1)^2/2\} \tag{8}$$

so as to get the transition rate described by the sum of the Gaussian-shaped n-photons resonance,

$$W_{01} = \sqrt{\frac{\pi}{8}}\frac{\Delta^2}{W}\sum_n J_n^2\left(\frac{A}{\omega}\right)\exp\left\{-\frac{[\varepsilon_0 - n\omega - \varepsilon_p(t)]^2}{2W^2}\right\}, \tag{9}$$

where $W^2 = \int d\omega' S(\omega')$, $\varepsilon_p(t) = \mathcal{P}\int d\omega \frac{S(\omega')}{\omega'}(1 - \cos\omega' t)$, and $\varepsilon_p(t)[\varepsilon_p(t) \neq 0]$ represents quantum component of low-frequency noise. Using similar procedure, we can also obtain the transition rate from $|1\rangle$ to $|0\rangle$ $W_{10}(\varepsilon_0) = W_{01}(-\varepsilon_0)$. These are the transition rates in the presence of strong low-frequency quantum noise. We define the character frequency ω_c under which the spectrum $S(\omega')$ possesses most of noise energy. For a typical ω_c, the contribution of low-frequency noise can be separated into three relevant regimes: (a) $\omega_c t \ll 1$, $\varepsilon_p(t) \approx 0$; (b) $\omega_c t \backsim 1$, $\varepsilon_p(t)$ shows oscillatory increase because of the sinusoidal time dependence of $\varepsilon_p(t)$; (c) $\omega_c t \gg 1$, the integral contains many oscillations of the sinusoidal function and therefore vanishes so $\varepsilon_p(t) = \varepsilon_{p0} = \mathcal{P}\int d\omega \frac{S(\omega)}{\omega}$. Therefore, $1/\omega_c$ represents the character time within which the quantum effect of the environment is effective. The discussions hereafter are focused in the regime (c) where $\varepsilon_p(t) = \varepsilon_{p0}$.

When $S(\omega')$ is symmetric in ω', $\varepsilon_p(t)$ may disappear and we have

$$W_{01} = W_{10} = \sqrt{\frac{\pi}{8}}\frac{\Delta^2}{W}\sum_n J_n^2\left(\frac{A}{\omega}\right)\exp\left\{-\frac{(\varepsilon_0 - n\omega)^2}{2W^2}\right\}. \tag{10}$$

This collapses to the result of low-frequency classical noise which is similar to Eq. (7) but with the sum of the Gaussian-shaped resonances. Comparing Eqs. (9) and (10), we find that quantum noise not only broadens the resonant peaks but also adds an additional energy detuning ε_{p0} to them. The quantum noise thereby shows remarkably different effects compared with that of the classical noise. The origin of the novel features comes from the extra off-diagonal factor $U_+^\dagger(t)U_-(t)$ in Eq. (2). $U_+^\dagger(t)U_-(t)$ moves the symmetric splitting Δ formed by $|0\rangle$ and $|1\rangle$ at the degeneracy point $\varepsilon = 0$ (Fig. 1) to energy detuning $A(\varepsilon = -\varepsilon_{p0})$ and $B(\varepsilon = \varepsilon_{p0})$, respectively[22] [Fig. 2(a)], with asymmetric transition rates W_{01} and W_{10}. At $A(B)$, only $|1\rangle$ ($|0\rangle$) can be split to the superposition of $|1\rangle$ and $|0\rangle$ while $|0\rangle$ ($|1\rangle$) is not split. That means A (B) is a beam splitter only working for $|1\rangle$ ($|0\rangle$). Furthermore, as seen from Eq. (8), under the strong low-frequency quantum noise $U_+^\dagger(t)U_-(t)$ produces a phase accumulation $i\varepsilon_{p0}t$, which influences the interference phase accumulation and the total phase accumulation. Therefore, quantum noise will modify the interference and resonant conditions.

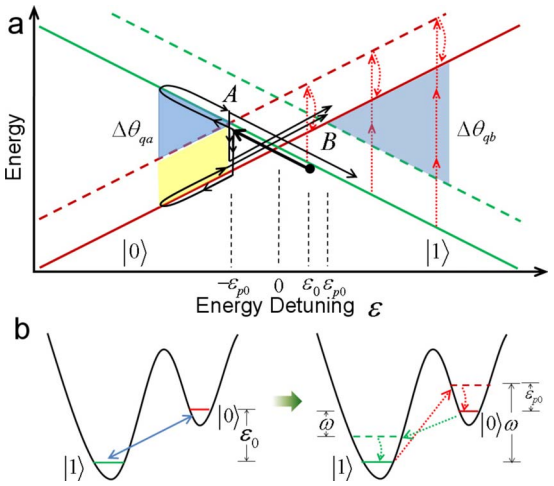

FIG. 2. (Color online) (a) Schematic energy diagram to generate "unconventional" Landau-Zener-Stückelberg interferometry in the presence of strong low-frequency noise. The dashed arrows mark the multiphoton resonant transition from $|1\rangle$ to $|0\rangle$. (b) Effectively, the noise changes the resonant condition $n\omega = \varepsilon_0$ to $n\omega = \varepsilon_0 + \varepsilon_{p0}$ ($|1\rangle$ to $|0\rangle$) and $n\omega = \varepsilon_0 - \varepsilon_{p0}$ ($|0\rangle$ to $|1\rangle$). For a microwave with fixed frequency, the flux biases resonant with $|1\rangle$ to $|0\rangle$ transition are usually far off resonant with $|0\rangle$ to $|1\rangle$ transition. Therefore, stationary population can build up in $|0\rangle$ state and generate population inversions at those flux biases.

Now we investigate the LZS interferometry in the low-frequency quantum noise [Fig. 2(a)]. The system is initialized in state $|1\rangle$ at $\varepsilon = \varepsilon_0$ (solid circle). Microwave sweeps the state along $|1\rangle$ (solid arrow). By reaching point A (time t_1) where $\varepsilon = -\varepsilon_{p0}$, $|1\rangle$ is split into the superposition of $|1\rangle$ and $|0\rangle$, collecting different phases in two paths. When they are driven back to A (time t_2), $|1\rangle$ is split into $|1\rangle$ and $|0\rangle$ again. However, different from the conventional LZS interferometry, $|0\rangle$ will not be split. Because A is not a beam splitter for $|0\rangle$. This is the key of the asymmetric LZ transition rates in Eq. (9). Evolving independently, $|1\rangle$ and $|0\rangle$ accumulate a relative phase difference $\Delta\theta_{qs}$, marked with the dark shade (blue online) region plus light shade (yellow online) region.

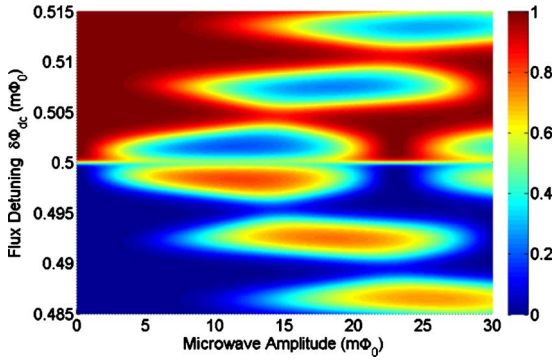

FIG. 3. (Color online) Three-dimensional view of the dependence of the population in the qubit level $|0\rangle$ in the right well as function of flux detuning and microwave amplitude. x, y, and z axes represent microwave amplitude, the qubit flux detuning, and the population in $|0\rangle$, respectively. Strong population inversion due to LZ transition is clearly demonstrated. Strong population inversion based on one-, two-, and three-photon absorption due to LZS interference is clearly observed. The parameters for the qubit are $\Delta/2\pi=0.1$ GHz and the microwave frequency $\omega/2\pi=15.9$ GHz, the temperature $T\approx 20$ mK, $\epsilon_{p0}/2\pi\approx 12$ GHz, $W/2\pi\approx 3$ GHz, and the interwell relaxation time $T_1\approx 1$ μs.

However, the effective phase difference contributing to the interference at A is $\Delta\theta_{qa}$ (blue region) since quantum noise eliminates part of the phase (yellow region). Then the qubit state is driven to point B and similar procedure happens, leading to an effective phase difference $\Delta\theta_{qb}$.

The interference phase caused by A is $\Delta\theta_{qa}=\int_{t_1}^{t_2}dt(\varepsilon_{|0\rangle}-\varepsilon_{|1\rangle}+\varepsilon_{p0})$, where $\varepsilon_{|1\rangle}=-\varepsilon(t)/2$, $\varepsilon_{|0\rangle}=\varepsilon(t)/2$. The total phase gained over one period referring to A is $\theta_A=\oint dt(\varepsilon_{|0\rangle}-\varepsilon_{|1\rangle}+\varepsilon_{p0})=2\pi(\varepsilon_0+\varepsilon_{p0})/\omega$. Similarly the total phase gained over one period referring to B is $\theta_B=\oint dt(\varepsilon_{|1\rangle}+\varepsilon_{p0}-\varepsilon_{|0\rangle})=2\pi(\varepsilon_0-\varepsilon_{p0})/\omega$. Consecutive pairs of LZ transitions interfere constructively when θ_A or $\theta_B=2\pi n$. Therefore, the resonant transition from $|1\rangle$ to $|0\rangle$ (from $|0\rangle$ to $|1\rangle$) will occur at $\varepsilon_0=n\omega-\varepsilon_{p0}(\varepsilon_0=n\omega+\varepsilon_{p0})$ [Fig. 2(b)]. The energy conservation is satisfied in the unconventional way for these transitions. For $|1\rangle$ to $|0\rangle$ [Figs. 2(a) and 3], n photons with frequency ω are absorbed. The total energy $n\omega=\varepsilon_0+\varepsilon_{p0}$ is larger than the energy ε_0 needed to excite the qubit. The excess energy ε_{p0} is flowing into the low-frequency environment. Similarly, the qubit emits n photons with energy $n\omega=\varepsilon_0-\varepsilon_{p0}$ and the excess energy ε_{p0} is also flowing into the low-frequency environment. In contrast, for a conventional LZS interferometry shown in Fig. 1, the paths may not be detoured and $\varepsilon_{p0}=0$ so that the resonant conditions of $|1\rangle\rightarrow|0\rangle$ and $|0\rangle\rightarrow|1\rangle$ are the same, just as described by the LZ transition rates in Eqs. (7) and (10). Then the unconventional LZS interferometry shown in Fig. 3(a) is described by the LZ transition rate in Eq. (9).

In order to get the stationary interference fringes in strong low-frequency noise, we employ a rate-equation approach considering the energy relaxation to the environment.[5] The level occupations $p_{0,1}$ obey $p_i=\Sigma_j m_{i,j}p_j$, where $m_{01}=-m_{11}=W_{01}+\Gamma_1'$, $m_{10}=-m_{00}=W_{10}+\Gamma_1$. $\Gamma_1=1/T_1$, and $\Gamma_1'=\Gamma_1 e^{-\beta\varepsilon_0}$ are the spontaneous down and up interwell relaxation rates between $|1\rangle$ and $|0\rangle$. The population of $|0\rangle$ is

$$p_0=\frac{W_{10}(\varepsilon_0)+\Gamma_1'}{W_{01}(\varepsilon_0)+\Gamma_1'+W_{10}(\varepsilon_0)+\Gamma_1}. \tag{11}$$

Using Eq. (11), we simulate the stationary population of $|0\rangle$ (Fig. 3), which exhibits not only the shift of the resonant peaks but also population inversion.

From Einstein AB coefficient theory, for a quantum TLS driven by rf electromagnetic field, the population in the lower state is always larger than that in the higher state at equilibrium. Therefore, the largest population in the higher state is 0.5. If the population in the higher state is larger than 0.5, population inversion happens. The population inversion has important application in laser. In general, more than two levels are usually required to generate population inversion.[6,13,14] However, It is interesting that the low-frequency quantum noise can produce the population inversion in TLS. For experiments at sub-Kelvin temperature ($\sim$20 mK),[3,5,7] the typical parameters of the two lowest levels in different wells are $\Delta/2\pi\approx 8-10$ MHz, $\Gamma_1\approx 1-0.05$ MHz, and $\Gamma_2\approx 2000-100$ MHz (the left and right boundaries of these parameters come from the same experiment). Therefore, $\Delta^2/W\gg\Gamma_1$. In this case when $\varepsilon_0=n\omega-\varepsilon_{p0}$, and the resonant condition from $|0\rangle$ to $|1\rangle$ is not fulfilled, at suitable microwave amplitude, Γ_1 and W_{01} are much smaller than W_{10}. Hence there will be less population transferred from $|0\rangle$ to $|1\rangle$, and a stationary population inversion will happen with p_0 larger than 0.5 and even close to 1 (Fig. 3). However, sometimes two resonance conditions are close, the transitions at A and B will influence the population transition together and the interference patterns will become complicated.

In a recent experiment,[7] LZS interference was observed in an rf superconducting quantum interference device. The fringe of interference patterns were different from the conventional LZS interference because the resonant peaks detuning values ε_n did not meet $\varepsilon_n\propto n$. Moreover, population inversion was observed. Considering the fact that the qubit is strongly subjected to the low-frequency noise due to large geometry size,[23–25] our theory provides a natural and possible explanation to the experimental results. As shown in Fig. 3, the simulated stationary population agrees well with the experimental results.[7]

We emphasize that population inversion described here differs from the "dress-state population inversion" proposed in quantum dot system and population inversion in other nomial TLS.[15–18] Here the unconventional LZS interferometry driven by the strong field serves as a tool to realize the population inversion. Therefore, we can control the population inversion by adjusting microwave amplitude, frequency, and energy detuning. In addition, the population inversion in our theory does not rely on the explicit structure of the environment bath and the spectral density. Therefore, it is easier to be implemented in superconducting systems and other TLS system, thus supplying a more convenient way for the application of lasing and microwave cooling. We also notice that the shift of the peaks of macroscopic resonant tunneling has been reported and used to diagnose the noise of superconducting qubits.[23,24] Actually, the resonant tunneling corresponds with zero power case of our theory.[22] With

microwave driving, the shift of the microwave resonant peaks can also be used to analyze the noise property. In general, microwave generated LZS interferometry is more robust than resonant tunneling. Furthermore, we can tune the frequency and amplitude of the microwave. The flexibility together with the higher resolution makes the LZS interference a better tool to diagnose the noise in qubits.

In summary, we have investigated unconventional LZS interferometry in the presence of quantum noise. The transition rate induced by consecutive LZ transitions is obtained, from which LZS interferometry can be analytically calculated based on rate equation. In the presence of significant frequency-dependent noise, the evolving paths for collecting phase difference are going to be detoured and the position of the resonant peaks is shifted. The resulted unconventional LZS interferometry can be formed and a stationary population inversion in TLS without involving the third qubit state is generated. The interferometry can be used to investigate the noise property hence the decoherence source of the system. In addition, the stationary population inversion may find application in lasing and microwave cooling.

We would like to thank M. H. S. Amin and X. D. Wen for helpful discussion. This work was supported by the State Key Program for Basic Researches of China (Grant No. 2006CB921801) and the NSFC (Grant No. 10725415).

*yuyang@nju.edu.cn

[1] L. D. Landau, Phys. Z. Sowjetunion **2**, 46 (1932); G. Zener, Proc. R. Soc. London, Ser. A **137**, 696 (1932); E. C. G. Stückelberg, Helv. Phys. Acta **5**, 369 (1932).
[2] S. N. Shevchenko, S. Ashhab, and F. Nori, Phys. Rep. **492**, 1 (2010).
[3] W. D. Oliver, Y. Yu, J. C. Lee, K. K. Berggren, L. S. Levitov, and T. P. Orlando, Science **310**, 1653 (2005).
[4] M. Sillanpää, T. Lehtinen, A. Paila, Y. Makhlin, and P. Hakonen, Phys. Rev. Lett. **96**, 187002 (2006).
[5] D. M. Berns, W. D. Oliver, S. O. Valenzuela, A. V. Shytov, K. K. Berggren, L. S. Levitov, and T. P. Orlando, Phys. Rev. Lett. **97**, 150502 (2006).
[6] D. M. Berns, M. S. Rudner, S. O. Valenzuela, K. K. Berggren, W. D. Oliver, L. S. Levitov, and T. P. Orlando, Nature (London) **455**, 51 (2008).
[7] G. Z. Sun, X. D. Wen, Y. W. Wang, S. H. Cong, J. Chen, L. Kang, W. W. Xu, Y. Yu, S. Y. Han, and P. H. Wu, Appl. Phys. Lett. **94**, 102502 (2009).
[8] A. J. Leggett, S. Chakravarty, A. T. Dorsey, M. P. A. Fisher, A. Garg, and W. Zwerger, Rev. Mod. Phys. **59**, 1 (1987).
[9] M. A. Nielsen and I. L. Chuang, *Quantum Computation and Quantum Information* (Cambridge University Press, Cambridge, 2000).
[10] Y. Makhlin, G. Schön, and A. Shnirman, Rev. Mod. Phys. **73**, 357 (2001).
[11] A. V. Shytov, D. A. Ivanov, and M. V. Feigel'man, Eur. Phys. J. B **36**, 263 (2003).
[12] X. D. Wen and Y. Yu, Phys. Rev. B **79**, 094529 (2009).
[13] S. Y. Han, R. Rouse, and J. E. Lukens, Phys. Rev. Lett. **76**, 3404 (1996).
[14] J. Q. You, Y. X. Liu, C. P. Sun, and F. Nori, Phys. Rev. B **75**, 104516 (2007).
[15] M. C. Goorden, M. Thorwart, and M. Grifoni, Phys. Rev. Lett. **93**, 267005 (2004).
[16] A. A. Clerk, S. M. Girvin, A. K. Nguyen, and A. D. Stone, Phys. Rev. Lett. **89**, 176804 (2002).
[17] T. M. Stace, A. C. Doherty, and S. D. Barrett, Phys. Rev. Lett. **95**, 106801 (2005).
[18] M. I. Dykman, Sov. J. Low Temp. Phys. **5**, 89 (1979).
[19] M. H. S. Amin and F. Brito, Phys. Rev. B **80**, 214302 (2009).
[20] The derivation from Eqs. (4)–(6) followed the procedures in Ref. 19.
[21] J. M. Martinis, S. Nam, J. Aumentado, K. M. Lang, and C. Urbina, Phys. Rev. B **67**, 094510 (2003).
[22] For classical noise, the resonant tunneling rate is Eq. (10) with $A=0$. At the degeneracy point where energy detuning is 0, both of the transition rates from $|1\rangle$ to $|0\rangle$ and from $|0\rangle$ to $|1\rangle$ are maximum. For quantum noise, the resonant tunneling rate (Ref. 23) is Eq. (9) with $A=0$. When energy detuning is $-\varepsilon_{p0}$ (ε_{p0}), the transition rate from $|1\rangle$ to $|0\rangle$ ($|0\rangle$ to $|1\rangle$) is maximum and the transition rate from $|0\rangle$ to $|1\rangle$ ($|1\rangle$ to $|0\rangle$) is very low. When energy detuning is 0, both rates are very low.
[23] M. H. S. Amin and D. V. Averin, Phys. Rev. Lett. **100**, 197001 (2008).
[24] R. Harris, M. W. Johnson, S. Y. Han, A. J. Berkley, J. Johansson, P. Bunyk, E. Ladizinsky, S. Govorkov, M. C. Thom, S. Uchaikin, B. Bumble, A. Fung, A. Kaul, A. Kleinsasser, M. H. S. Amin, and D. V. Averin, Phys. Rev. Lett. **101**, 117003 (2008).
[25] T. Lanting, A. J. Berkley, B. Bumble, P. Bunyk, A. Fung, J. Johansson, A. Kaul, A. Kleinsasser, E. Ladizinsky, F. Maibaum, R. Harris, M. W. Johnson, E. Tolkacheva, and M. H. S. Amin, Phys. Rev. B **79**, 060509 (2009).